LEGIBILITY NOTICE

A major purpose of the Technical Information Center is to provide the broadest dissemination possible of information contained in DOE's Research and Development Reports to business, industry, the academic community, and federal, state and local governments.

Although a small portion of this report is not reproducible, it is being made available to expedite the availability of information on the research discussed herein.

LA-UR-88-2439

LA-UR--88-2439

DE88 014394

TITLE: CALCULATION OF SUBSEQUENT STRUCTURAL EFFECTS AFTER AN ACCIDENTAL EXPLOSION IN A TEST FACILITY

AUTHOR(S): L. Erik Fugelso
Major Michel Deeter

SUBMITTED TO: 23rd DOD Explosives Safety Seminar
Atlanta, GA
Aug. 9-11, 1988

Calculation of Subsequent Structural Effects
After An Accidental Explosion in a Test Facility

L. Erik Fugelso[1]
Major Michel Deeter[2]

Advanced Engineering Technology Group
Los Alamos National Laboratory
University of California
Los Alamos, NM 87544

INTRODUCTION

This paper presents an analysis of the deformation and potential damage to a critical component of an experiment at the flame source in a high intensity burner due to a small accidental explosion. First, the accident is briefly summarized. Then, upper and lower bounds for the explosive load are estimated. Next, a finite element model of one of the the key structural components is generated and the simplifying assumptions are critically evaluated. Then the results of the appropriate finite element calculation are evaluated and the effect of the accident on the structure is presented.

DESCRIPTION OF THE PROBLEM

The experimental test fixture that serves as the source of a high intensity flame consists of four burners, two liquid oxygen (LOX) tanks, four gaseous nitrogen tanks, four tanks filled with powdered aluminum, the requisite connecting tubes, control hydraulics and electronic controls. Figure 1 shows a highly idealized and simplified schematic drawing of a typical section of the test fixture. Powdered aluminum is added by gravity feed to a gaseous nitrogen flow and transported through a pipeline into the center of a mixing nozzle. Liquid oxygen flows through another pipeline into the exterior annulus of this mixing nozzle of the burner, where the oxygen is vaporized. The coaxial streams of gas and aluminum powder mix and form a highly combustible mixture that is ignited by a pilot light. This system creates a vertical plume of a burning mixture with thermal flux properties that can be readily controlled with respect to heat flux intensity, duration and areal extent. Upon completion of each test, the mixing chambers are flushed with their respective inlet gases. When the system is restarted, there is a period of initial gas flow to flush the system of any residual fuel.

One test run was made with a much finer aluminum powder (6μ nominal particle size) to investigate the effect of increased surface area of the dispersed fuel on the thermal flux. The next test was to be done with the normal size (18μ nominal particle size) aluminum powder. During the initial O_2 flush of the mixing chambers, a small explosion took place. No aluminum powder had yet been added to the flow. The exterior annular walls of the mixers were blown off and visual flashes were noted at the two inner burners. Visual examination of the damaged exterior showed scorch marks on the support stands. The nearby liquid oxygen tank is mounted within a large volume of thermal insulation and could not be conveniently examined. This tank is connected to the mixing chamber through a flexible pipe. The explosion was caused by a small amount of unburned very fine aluminum powder that had fallen back into the exterior annulus of the mixing chamber at the termination of that run and that had not been removed by the previous gas flush or by the mechanical cleaning of the apparatus.

The mixer and the external piping systems can be visually examined and quickly repaired or replaced as necessary. Since the liquid oxygen tank and the piping system internal to the thermal insulation cannot be conveniently examined, a finite element calculation was performed to determine whether further inspection of this component was necessary.

METHOD OF APPROACH

We examine in detail the potential structural deformation in the liquid oxygen tank from this event. Upper and lower bounds on the explosive energy release in the mixing chamber are obtained. The transmission of this energy along the connecting tubes is examined. Finally a structural analysis of the stresses and displacements in the liquid O_2 tank was carried out using a finite element analysis, which incorporated a constitutive material model describing work-hardening plasticity to match the behavior of stainless steel at the cryogenic operating temperatures.

BOUNDS ON THE ENERGY RELEASE

We wish to establish a good estimate of the transient load that was incident on the liquid oxygen tank. The blast load will originate at the mixer and then be propagated through the connecting tubes. Thus we will first present the upper and lower bound of the energy released at the mixer. The upper bound on the energy release is obtained by assuming that the mixing chamber was completely filled with pure oxygen at STP and that sufficient aluminum powder was present on the interior surfaces of the mixing chamber to generate a stochiometric reaction. The volume of the annulus is 280 cm^3 (17 in^3), which would contain 0.40 gm or 0.0125 moles of O_2 at STP. The surface area of the annulus is 265 cm^2 (41 in^2). The volume of Al powder to stoichiometrically react with the oxygen will form a layer 6.3 μ thick. The heat of formation for this reaction is 400 kcal/mol of O_2. This heat release was equated to the detonation energy of an equivalent weight of TNT. The amount of TNT equivalent is 23 gm (0.047 lb). Distributing the blast effects in an equivalent sphere and evaluating the resulting blast pressure at its radius yielded a peak side-on pressure at the location where the oxygen inlet tube is attached of 12.4 MPa (1750 psi) (Baker et. al., 1980). This estimate required the unlikely combination of 100% efficiency of the reaction and uniform coverage of all interior surfaces by the aluminum powder. We reduced our estimate of the energy release slightly to account for this reduction in the total reaction efficiency. Thus the upper bound estimate used here is 10.3 MPa (1500 psi).

The lower limit on the explosion pressure was obtained by calculating the minimum internal pressure required to effect the the observed failure pattern in the annular wall of the mixing chamber. The annular wall of radius 6.35 cm (2.5") is 0.64 cm (0.25") thick. The inlet hole from the liquid oxygen line is 3.81 cm (1.5") in diameter. The failure pattern was a tensile in response to the circumferential tension in the narrow strip between the cutout and the top and bottom edges of the annulus (Figure 2). Using the stress concentration factor from Savin (1961) and a typical ultimate stress for aluminum, we obtain a lower bound of 3.1 MPa (450 psi) for the internal pressure.

ANALYSIS OF THE STRESSES IN THE LOX TANK

The loaded components of the system consist of the liquid oxygen tank and the pipe sections (Figure 3). The tank is held in an aluminum container that provides for handling as well as the insulation of the tank. The tank walls and the piping from the tank to the support structure are type 304 stainless steel. The two stainless steel pipe segments from the tank are symmetrically offset from the center of the torospherical cap. Each pipe segment has a 90° elbow between the cap and the exterior support structure. The piping exterior to the structure is flexible copper tubing. The temperatures of the tank and of the piping interior to the support structure are maintained at the boiling temperature of liquid oxygen , -183 C (-297 F). The initial internal pressure of the tank is 1.03 MPa (150 psi).

The pressure pulse that is felt at the oxygen tank is transmitted though the fluid contained in about 2 m of flexible copper tubing and the inner stainless steel tubing. The liquid oxygen was flowing at the time of the incident at a velocity of about 0.4 m/s. The blast load is assumed to be a rectangular pulse, the duration of which is determined by the largest interior dimension of the mixing chamber. This upper bound blast pressure in the mixing chamber generates an acoustic pulse propagating backwards in the pipe that, by Joukowsky's formula (Nekrosov 1969) is just sufficient to stop the flow. The pressure in the pipe is transferred to the pipe structure itself at the elbow. The magnitude of the static applied load is equal to the upper bound pressure times the cross section area of the pipe. This load is applied normal to the plane containing the tank axis and the centerlines of the two attached pipes. The "water hammer" model presented here describes a pulse that will traverse the length of the tube essentially unaltered. Estimates of pressure losses due to wall friction, viscosity, pipe curvature, wave reflection at any bends, N-wave dispersion, and acoustic radiation into the surround air or thermal insulation were made and, collectively, the decrement in the shock pressure jump is less than 10% of the initial value. These losses are thus ignored to remain conservative.

There is one load reduction factor that should not be ignored. The pressure pulse in the pipe has a very short duration that is small compared to the lowest period of vibration of the tank. Thus only a small fraction of the applied force will be activated. For structural motion calculations on a single-degree-of-freedom system a dynamic load factor (DLF) is defined, for a rectangular pulse of duration, t, by (Norris et. al., 1959)

$$DLF = 2 \sin(\pi t / T) ,$$

where T is the period of the single-degree-of-freedom structure. The dynamic load factor is the number by which the deflection, that is produced by a static load, is multiplied to obtain the dynamic deflection. For this problem, the pulse duration is about 3×10^{-5} , the fundamental period of the tank is about 3×10^{-3} and, thus, the dynamic load reduction factor is 0.06.

The stresses that might be expected in the liquid oxygen tank were calculated using the commercial finite element code, ABAQUS (Hibbett, Karlsson and Sorenson (1978). The assumptions for this calculation are made in a conservative manner such that the reported results are a "worst case" scenario. The first assumption is that the pressure wave reaches the external pipe - LOX tank connection unchanged in both magnitude and shape. Pressure pulse losses will probably occur due to shock transmission to the air and to the flexible hosing and due to friction at the liquid-pipe interface. Estimates of the pressure drop in an acoustic mode (e. g. Nekrasov 1969) and in an incompressible waterhammer mode (Parkmakian 1963) suggested that these loss mechanisms would be of the order of 10 to 20% for the transmitted impulse. The second assumption is that the welded connections between the tank head and the exit pipes have no fillets or thickened regions. Further, the angles of the joints are not rounded by the welding material. This is a conservative assumption because most welded joints will exhibit some material thickening at the joint and the rounding off of the sharp angles there. An additional assumption is that the loads are borne solely by the tank itself. In reality, some of the load will be absorbed by the external supporting structure, for example, through deformation of the aluminum wall at the pipe exit supports or by permanent deformation or compaction of the thermal insulation. Also a portion of the blast energy is contained in the kinetic energy of a back flow in the liquid oxygen stream. Some portion of this load will not be picked up by the elbow but will initiate a sound pulse into the liquid contents in the tank and, thus dispersed, will be involved with the short-time tank deformation considered here. We ignore this contribution.

The finite element mesh for one quarter of the structure is shown on Figure 4. The LOX tank has two off-center exit tubes (one of which is shown on this drawing). The tank itself is modeled as a thin cylindrical shell with a torospherical head. The tank is subjected to the initial internal pressure of 1.03 Mpa (150 psi) followed by the blast pressure. The blast load in the flowing oxygen stream is a rectangular pulse with a constant pressure equal to the upper bound limit. The total force is the product of the pressure times the cross-section area. This load is transferred to the inlet pipe at the 90° elbow (only one side of the elbow is shown) and is represented by a tangential force of 800 N (3600 lbs) applied at the top of the pipe stem. The static equivalent tangential load that is applied to the tank and pipe connector system is the above load multiplied by the dynamic load reduction factor appropriate to this problem and is 48 N (216 lbs).

An elastic analysis showed that the elastic limit conditions was exceeded in a very small region near the pipe-tank head juncture. An elastic-plastic analysis using a von Mises yield condition and including work hardening to fit the experimental stress-strain curve for type 304 stainless steel at -183 C was used. Figure 5 shows the contours of the maximum octahedral stress for the entire structure. A detail of this stress component near the pipe-tank juncture is shown in Figure 6. The stress concentration is just at yield at the juncture. Consideration of the maximum strain component at that point (shown of Figure 7) shows that the material is still well below ultimate as only 16% of the available plastic work was used. This excursion beyond yield was confined to a very small region.

CONCLUSIONS

The oxygen tank was loaded by a pressure pulse that was transmitted along the fluid in the piping system between the mixing chamber and the tank. The pressure signal that reached the tank should be low enough not to cause any damage. The worst case combination of loads, pipe losses, etc., in the system could generate a load at the tank that would result in a very localized region wherein the stresses were above yield but were well below the ultimate capacity. At the more probable lower limit, the response of the tank would be well below the proportional limit.

[1] Staff Member.

[2] Visiting Staff Member, Formerly, Asst. Prof., U.S. Army Military Academy, West Point, NY. Currently, HHB, 8th Btn, 8th FA, APO, San Francisco, CA.

REFERENCES

Baker, W. E., J. J. Kulasz, R. S. Westine, P. A. Cox and J. S. Wilbeck, "A Manual for the Prediction of Blast and Fragment Loadings on Structures," Technical Report, DOE/TIC-11268, Southwest Research Institute, (1980).

Hibbitt, Karlsson and Sorenson, Inc., ABAQUS, User's Manual, paged in sections, (1978).

Nekrosov, B., Hydraulics for Aeronautical Engineers, Trans. V. Talmy, MIR Publishers, Moscow, 295 pp., (1969).

Norris, C. H., R. J. Hansen, M. J. Holley, Jr., J. M. Biggs, S. Namyet, and J. K. Minami, Structural Design for Dynamic Loads, McGraw-Hill NY,453 pp., (1959).

Parmakian, J., Waterhammer Analysis, Dover, NY, 161 pp., (1963).

Savin, G. N., Stress Concentrations Around Holes, Trans. E. Gros, Pergamon Press, NY, 480 pp., (1961).

Figure 1. Schematic Diagram of the Test Apparatus

Figure 2. Fracture Pattern in the Deformed Annular Shell

Figure 3. Schematic Diagram of the Liquid Oxygen Tank, Internal Piping and Support Structure

Figure 4. Finite Element Mesh of the Liquid Oxygen Tank

Figure 5. Contours of the Octahedral Stress, von Mises Elastic-Plastic Model with Work-Hardening, Type 304 Stainless Steel at -18: C, 48 N Applied Tangentially to the Pipe Stub and Normal to the Symmetry Plane That Includes Both Pipe Stubs

Figure 6. Detail of Figure 5 Near the Pipe-Shell Cap Junction

Figure 7. Stress-Strain Curve for Type 304 Stainless Steel Showing the Plastic Work Done at the Location of Maximum Deformation

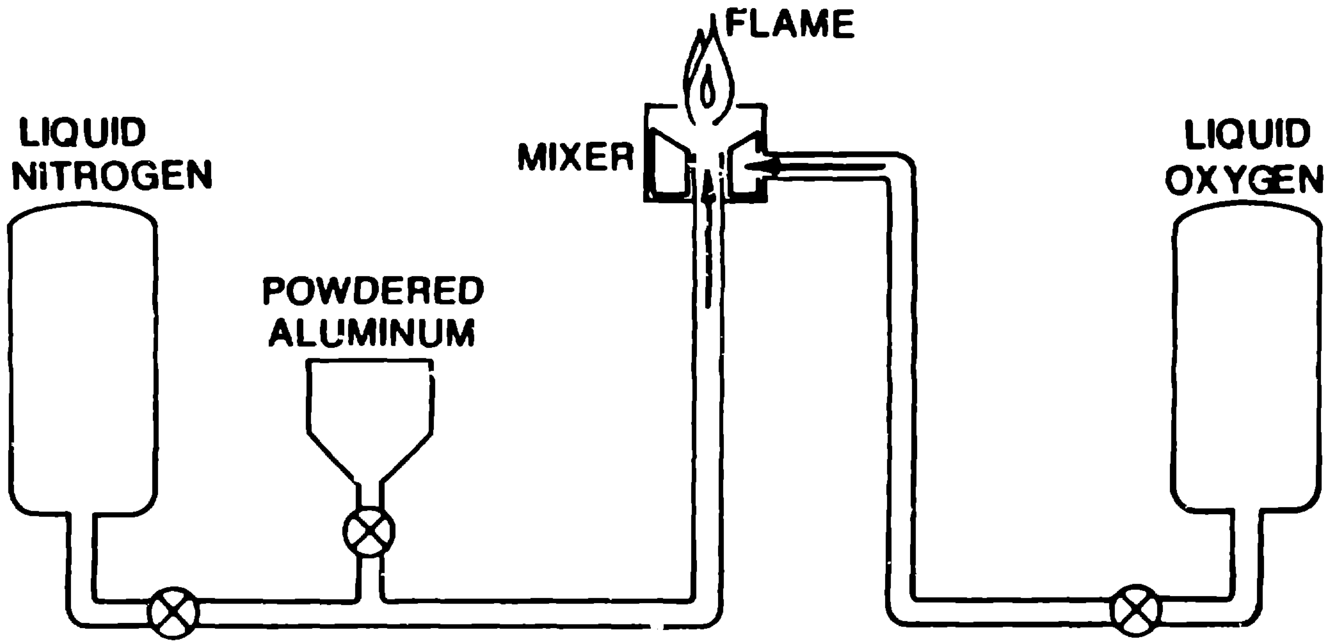
FLAME
LIQUID NITROGEN
MIXER
LIQUID OXYGEN
POWDERED ALUMINUM

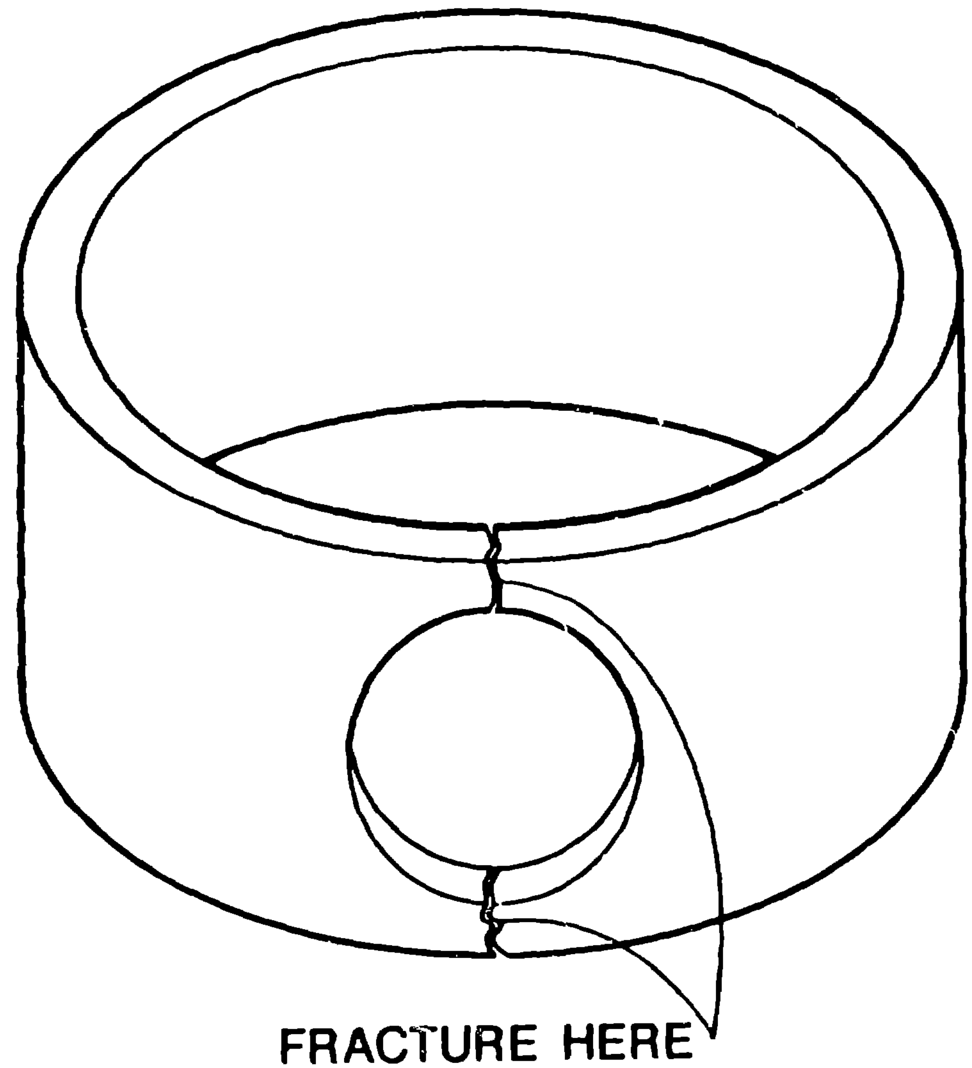

FRACTURE HERE

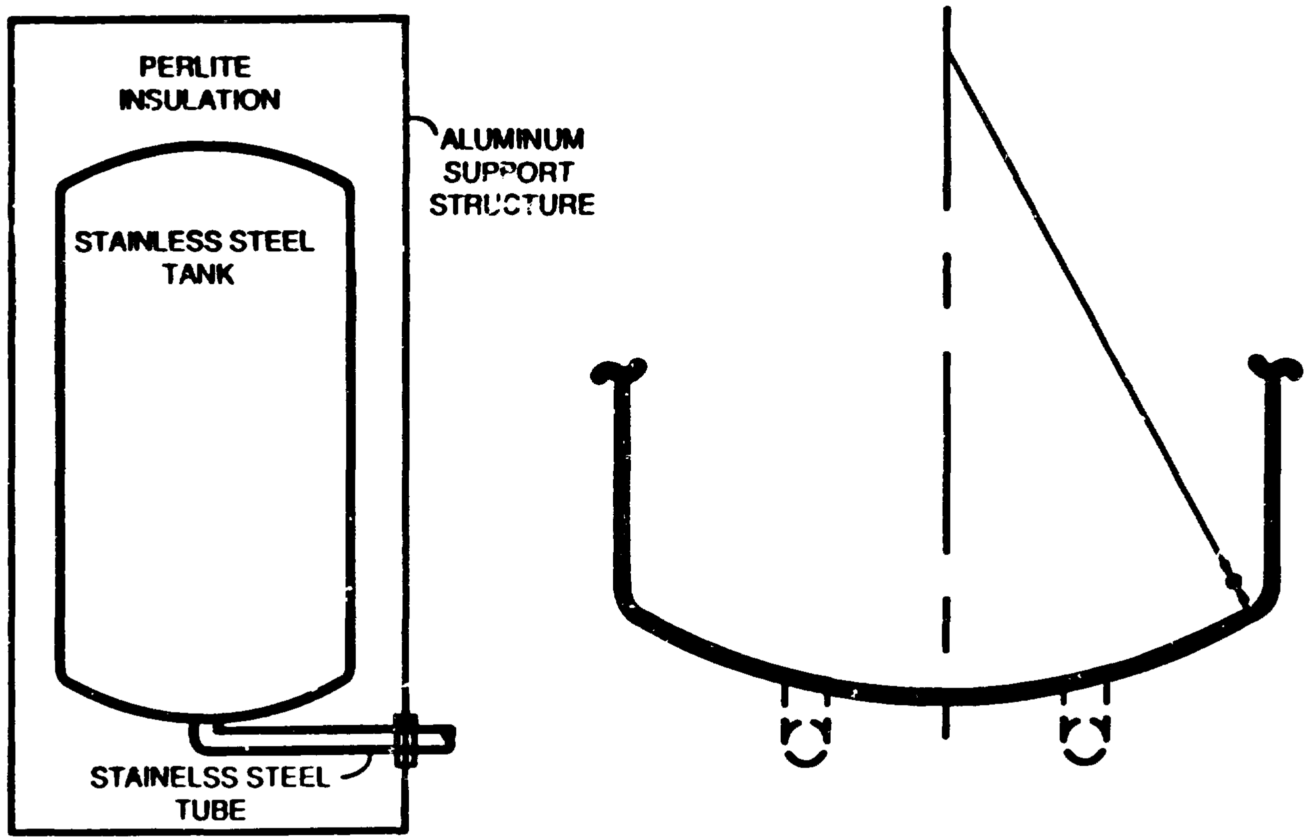
PERLITE
INSULATION
ALUMINUM
SUPPORT
STRUCTURE
STAINLESS STEEL
TANK
STAINELSS STEEL
TUBE

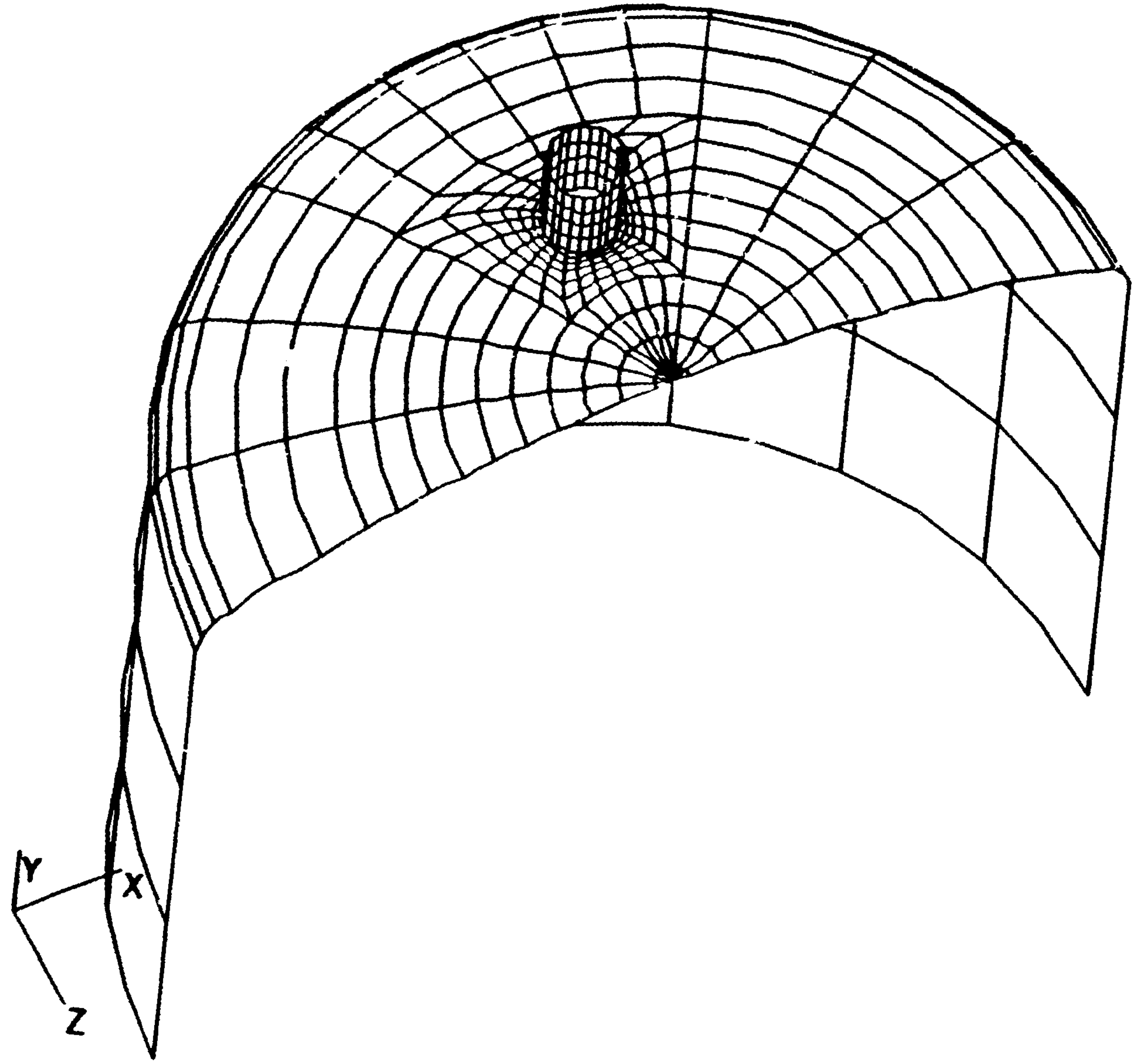
Y
X
Z

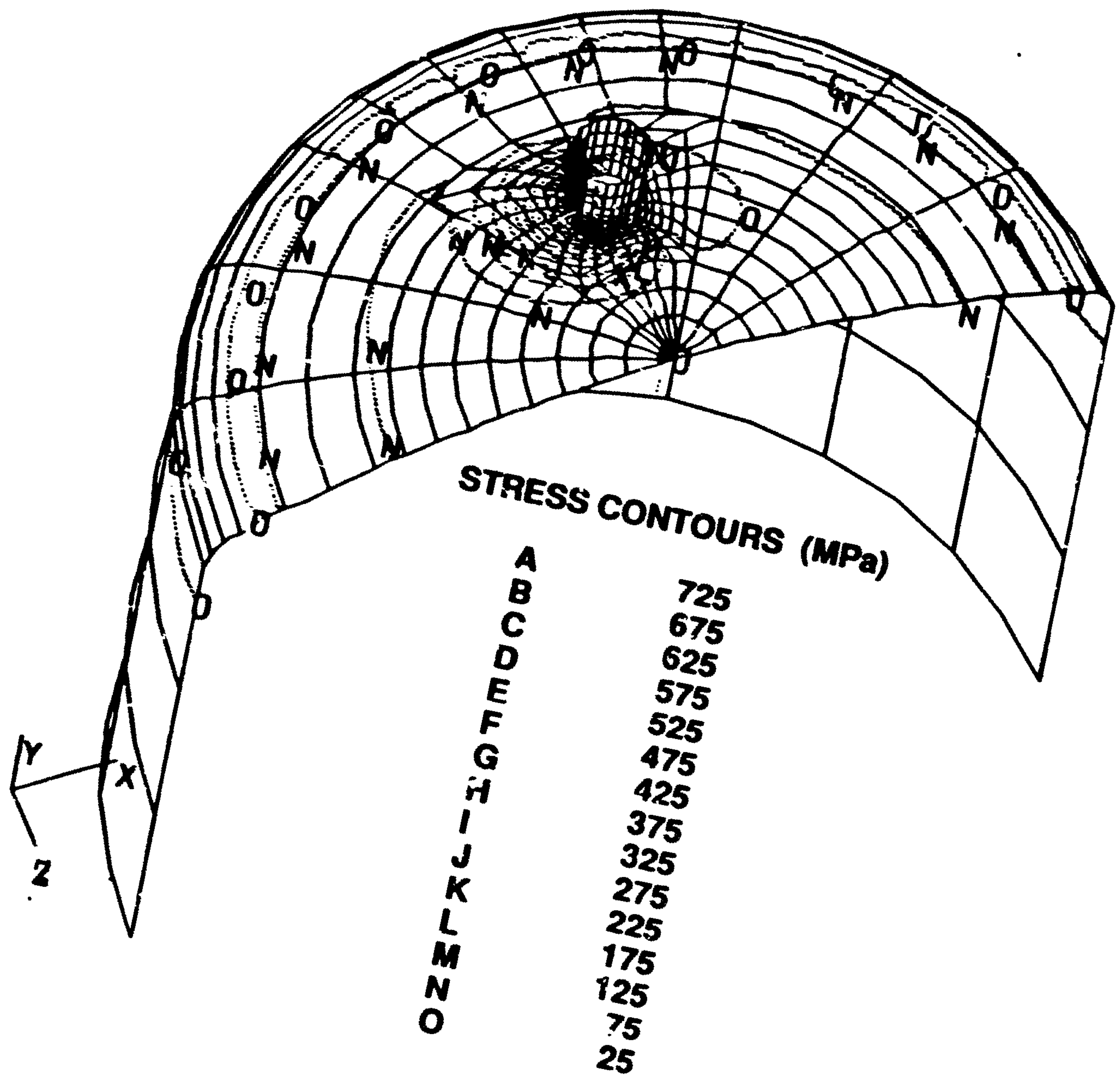
STRESS CONTOURS (MPa)
A 725
B 675
C 625
D 575
E 525
F 475
G 425
H 375
I 325
J 275
K 225
L 175
M 125
N 75
O 25
Y
X
Z

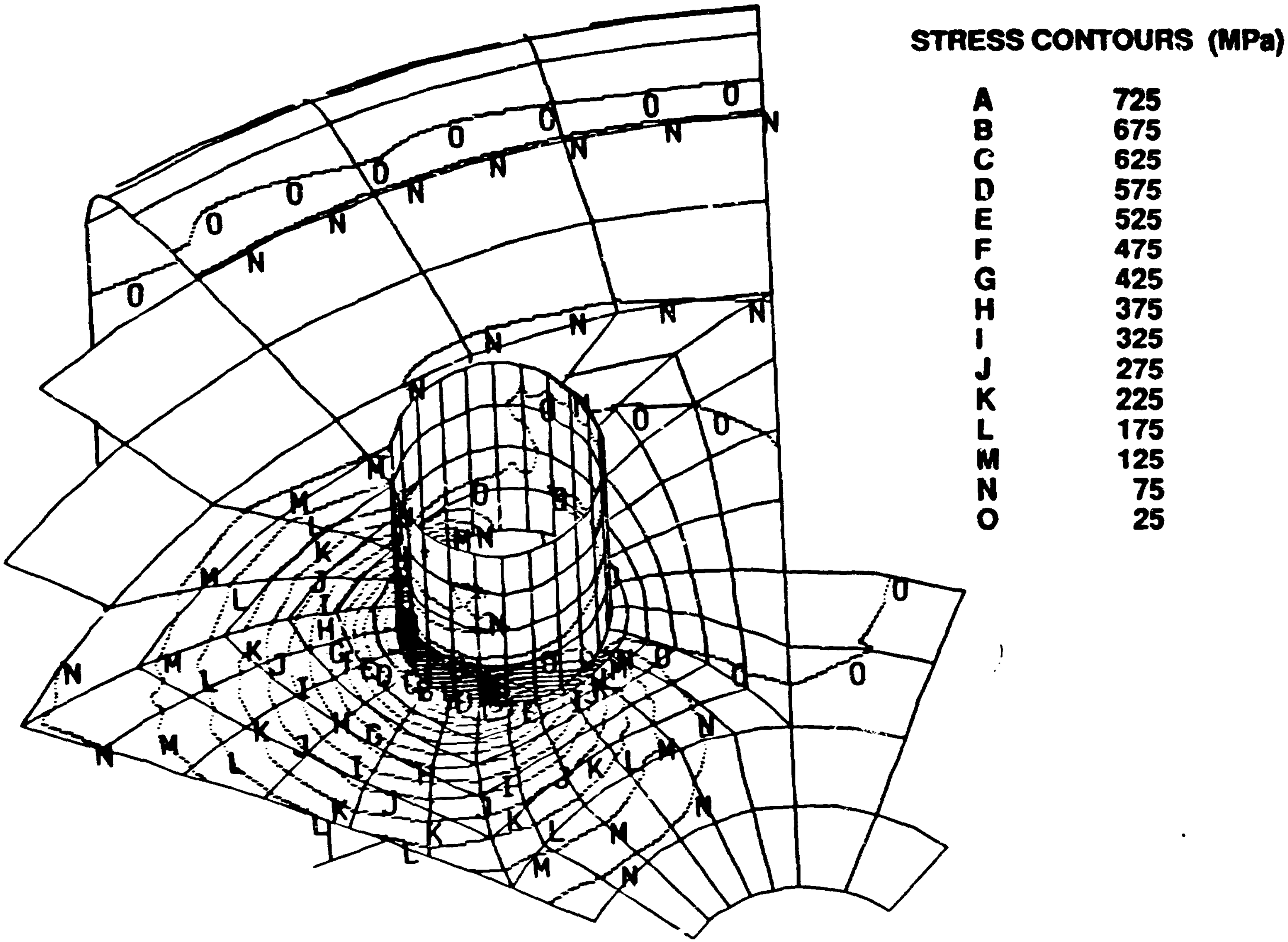
STRESS CONTOURS (MPa)
A 725
B 675
C 625
D 575
E 525
F 475
G 425
H 375
I 325
J 275
K 225
L 175
M 125
N 75
O 25

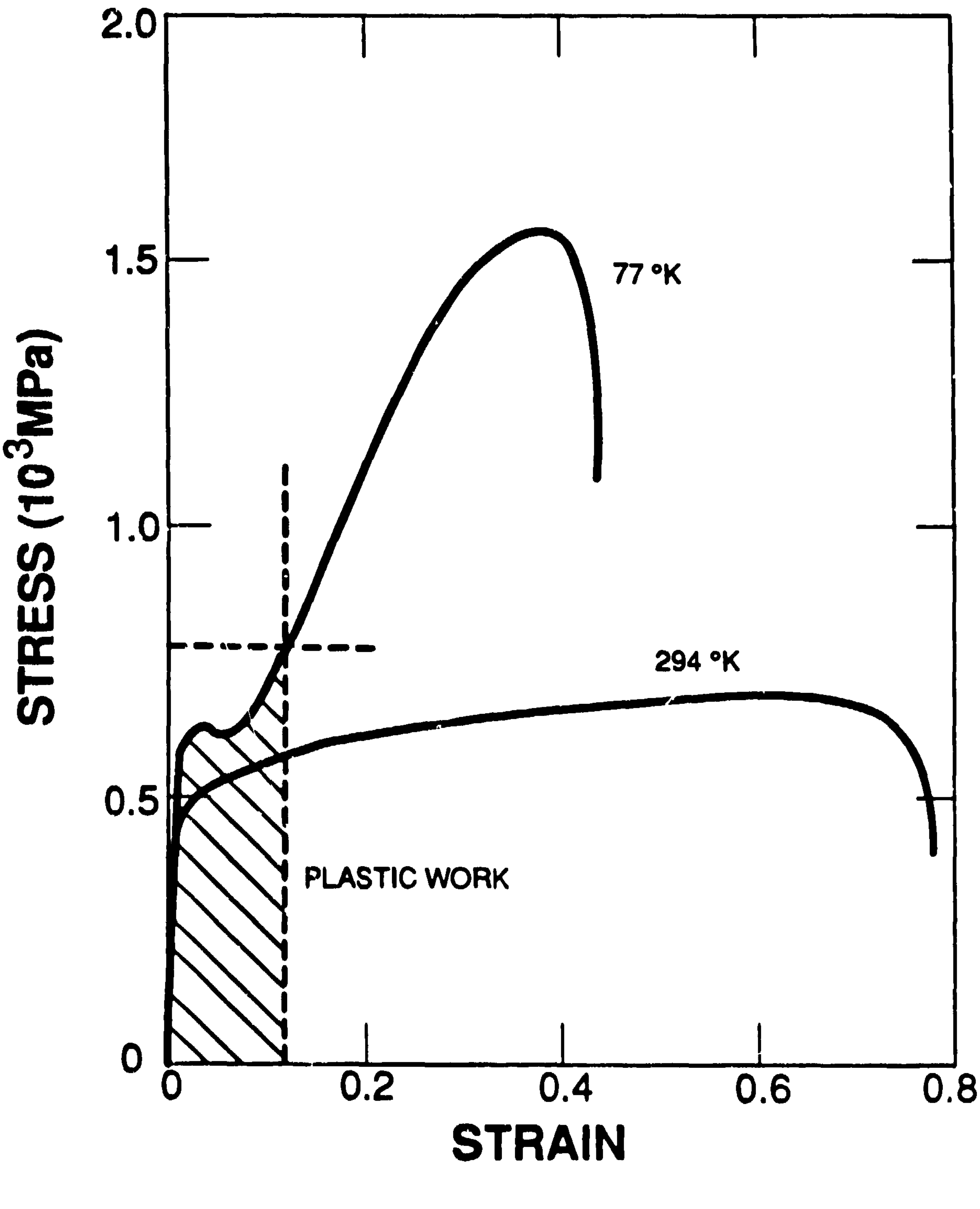

STRESS (10^3MPa)
2.0
1.5
1.0
0.5
0
77 °K
294 °K
PLASTIC WORK
0
0.2
0.4
0.6
0.8
STRAIN